

# NJC

Accepted Manuscript



This is an *Accepted Manuscript*, which has been through the Royal Society of Chemistry peer review process and has been accepted for publication.

*Accepted Manuscripts* are published online shortly after acceptance, before technical editing, formatting and proof reading. Using this free service, authors can make their results available to the community, in citable form, before we publish the edited article. We will replace this *Accepted Manuscript* with the edited and formatted *Advance Article* as soon as it is available.

You can find more information about *Accepted Manuscripts* in the [Information for Authors](#).

Please note that technical editing may introduce minor changes to the text and/or graphics, which may alter content. The journal's standard [Terms & Conditions](#) and the [Ethical guidelines](#) still apply. In no event shall the Royal Society of Chemistry be held responsible for any errors or omissions in this *Accepted Manuscript* or any consequences arising from the use of any information it contains.

## Bis - EDOT end capped by *n*-hexyl or *n*-hexylsulfanyl groups: Effect of the substituents on the stability of the oxidized states.

Mathieu Turbiez<sup>b</sup>, Djibril Faye,<sup>a</sup> Philippe Leriche,<sup>a\*</sup> and Pierre Frère<sup>a\*</sup>

a) University of Angers, MOLTECH-Anjou UMR CNRS 6200, 2 boulevard Lavoisier, 49045 Anger cedex, France

b) BASF Scheiwe AG, Schwarzwaldallee 215, CH-4002 Basel, Switzerland

### Summary

Three bisEDOT derivatives end capped with *n*-hexyl or *n*-hexylsulfanyl groups have been synthesized. The oxidation processes of these compounds have been studied by cyclic voltammetry and UV-Vis-NIR spectroscopy. The strong influence of the sulfur atoms of the hexylsulfanyl chains for stabilizing the oxidation states is evidenced. Thus, it is shown that the two compounds grafted with one or two hexylsulfanyl groups are reversibly oxidized into cation radical and dication states. By contrast compound end capped with hexyl groups present a fast  $\sigma$ -dimerization of the radical cation. The reduction of the  $\sigma$ -dimer to give the neutral bisEDOT derivative is slow.

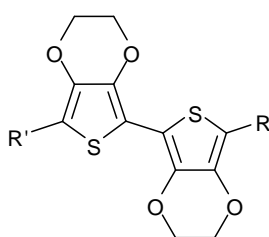
### Introduction

Due to their potential technological applications in the field of electronic plastics, thiophene-based conjugated oligomers represent one of the most widely investigated classes of functional  $\pi$ -conjugated systems.<sup>1-3</sup> For oligothiophene derivatives, the nature of substituents grafted on thiophene moieties contributes to modify the redox properties of the conjugated systems by acting directly on the HOMO and LUMO levels of the molecule.<sup>4-8</sup> 3,4-ethylenedioxythiophene (EDOT) is an efficient electron-rich building block largely used for tailoring the electronic properties of organic semiconductors for applications such as low band gap materials, electrochromic materials or organic solar cells.<sup>9-17</sup> The strong interest of the EDOT units to build various conjugated systems results of the combination of two effects: (i) the strong donating ability of the ethylenedioxy group, (ii) the propensity of EDOT to develop noncovalent intramolecular S...O interactions with adjacent thiophenic units that rigidify the conjugated systems.<sup>18</sup>

The electronic and geometrical effects of the substituents end capping oligothiophene derivatives can also modify the stability of the oxidized species by inhibiting or by favouring the coupling reaction of the radicals. Thus in 1996, Miller and *coll* showed that thiophene or

bithiophene units end capped by alkylsulfanyl groups presented highly stable cation radical and dication states.<sup>19</sup> Hicks and *coll* described the formation of stable oxidized states for oligothiophenes substituted in terminal positions by mesitylsulfanyl groups.<sup>20, 21</sup> Authors interpreted this result as the concomitant important participation of the sulphur atoms in the delocalization of the positive charges and steric effects due to the mesityl groups. By contrast for bis-EDOT end capped by hexyl substituents, a rapid evolution of the cation radical which prevented the subsequent formation of dication was observed.<sup>22, 23</sup> Analogous evolutions were described by Miller et al. on oligothiophenes bearing both methyl groups on the terminal  $\alpha$ ,  $\alpha'$  positions and methoxy groups on the  $\beta$ ,  $\beta'$  positions.<sup>24</sup> The authors indicated that the resulting radical cations first evolved to alcohol by loss of a proton and reaction with water, and then were quickly oxidized to aldehyde without however clearly demonstrating the presence of these compounds.<sup>24</sup> An electrochemical study carried out by Heinze and *coll* on similar compounds contradicted the previous conclusions as these later postulated the formation of  $\sigma$ -dimers by coupling of the radicals.<sup>25-27</sup> The dicationic species then obtained were reducible to give the monomer back but applying potentials lower than those corresponding to oxidation. In oligothiophene series,  $\sigma$ -dimers have never been isolated but different systems with analogous chemical properties have been isolated.<sup>28, 29</sup>

In the continuation of our current interest in conjugated systems based on EDOT moieties, we report here on the effect of the n-hexyl and n-hexylsulfanyl groups on the electronic properties of bis-EDOT derivatives **EEa-c** (Chart 1) and we show the impact of the sulphur atom on the stability of the oxidized species.



**EEa** : R = R' = -C<sub>6</sub>H<sub>13</sub>

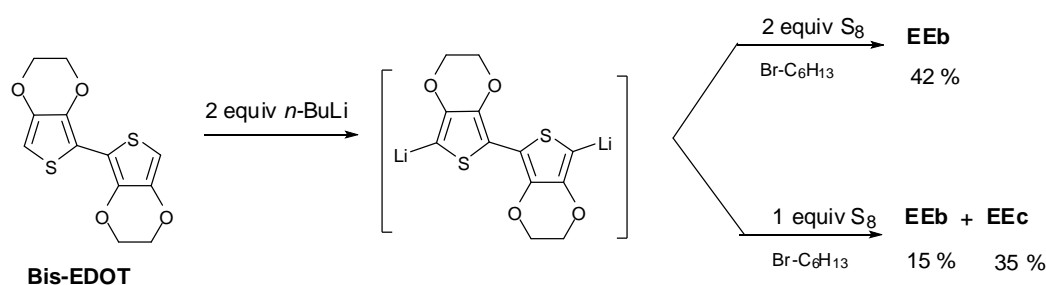
**EEb** : R = R' = -SC<sub>6</sub>H<sub>13</sub>

**EEc** : R = -SC<sub>6</sub>H<sub>13</sub> and R' = C<sub>6</sub>H<sub>13</sub>

Chart 1

## Results and discussion

Compound **EEa** end capped by two *n*-hexyl chains was synthesized as already described.<sup>22</sup> The hexylsulfanyl groups were grafted on the bis-EDOT unit by the sequence BuLi/S followed by the addition of a slight excess of bromohexane as shown in scheme 1. Thus, the bis-lithiated derivative of bis-EDOT afforded **EEb** in 42% yield. The use of one equivalent of sulphur on the dilithiated bis-EDOT followed by the addition of an excess of bromohexane led to a mixture of **EEb** and **EEc** in 15% and 35% yield respectively.



**Scheme 1:** Syntheses of the dimers

The crystallographic structure of single crystals of **EEb** obtained by slow evaporation of chloroform – ethanol solutions were analyzed by X-ray diffractions. Compound **EEb** were crystallized in the triclinic P-1 space group. As shown in Figure 1, the two EDOT moieties adopt a planar anti-conformation with a dihedral angle close to 5°. The S---O distances of 2.93 Å are shorter than the sum of the van der Waals radii of sulfur and oxygen atoms which is characteristic for non covalent S---O intramolecular interactions leading to the self-planarization of the  $\pi$ -conjugated system.<sup>9, 18</sup> The molecules stack along the *a* axis and are shifted each other what limits steric interactions between the hexyl chains and leads to distances separating two planes defined by the EDOT moieties about 3.80 Å. Consequently, the shorter sulfur-sulfur contacts only attain  $d_{S\cdots S} = 3.957(1)$  Å distances (presented in blue dotted lines in the Figure 1b what corresponds to weak intermolecular interactions in the crystals. Along the *c* axis the columns of molecules are in contact by lipophilic interactions between the alkyl chains.

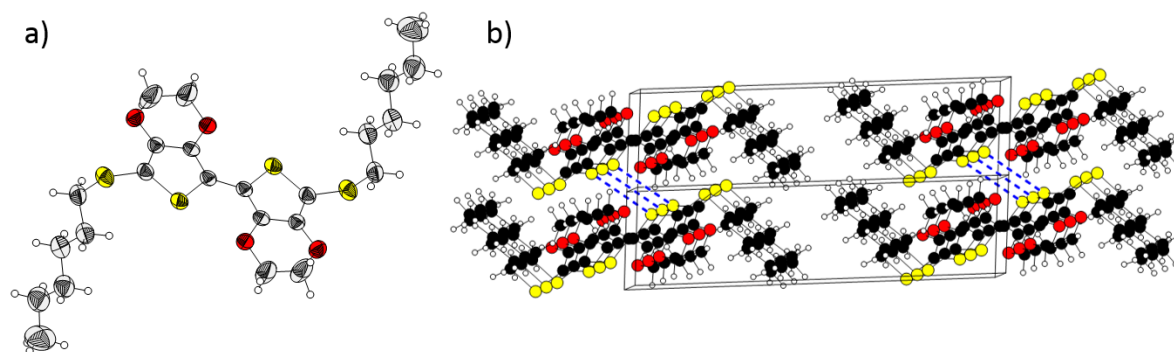


**Figure 1:** X-ray structure of compound **EEb**: a) Molecular structure of **EEb** with anisotropic displacement ellipsoids drawn at the 50% probability level; b) Stacking mode of the molecules in the crystal.

The electronic properties of compounds **EEa-c** were evaluated by theoretical calculations and analyzed by UV-Vis spectroscopy and by cyclic voltammetry. The theoretical and experimental data are gathered in Table 1.

**Table 1** HOMO and LUMO energy levels, theoretical bandgap  $\Delta E$  calculated by DFT methods,<sup>a</sup> experimental absorption data<sup>b</sup> and cyclic voltammetry data<sup>c</sup> of compounds **EEa-c**

Compd	HOMO <sup>a</sup> (eV)	LUMO <sup>a</sup> (eV)	$\Delta E_{\text{theo}}^a$ (eV)	$\lambda_{\text{max}}^b$ (nm)	$\lambda_{0-0}^b$ (nm)	$\Delta E_{\text{opt}}^d$ (eV)	$E_{\text{ox1}}^c$ (V)	$E_{\text{ox2}}^c$ (V)
<b>EEa</b>	-4.57	-0.68	3.89	333	349	3.55	0.65	-
<b>EEb</b>	-4.96	-1.23	3.73	350	367	3.37	0.74	0.89
<b>EEc</b>	-4.78	-0.98	3.80	344	361	3.43	0.70	1.00

<sup>a</sup> B3LYP/6-31G(d,p). <sup>b</sup>  $2 \cdot 10^{-5}$  M in  $\text{CH}_2\text{Cl}_2$ . <sup>c</sup>  $10^{-3}$  M in 0.1 M  $\text{Bu}_4\text{NPF}_6/\text{CH}_2\text{Cl}_2$ , scan rate 100  $\text{mVs}^{-1}$ . <sup>d</sup> Optical gap calculated from the lowest energy band  $\lambda_{0-0}$ .

Theoretical calculations were performed at the *ab initio* density functional level with the Gaussian09 package. Becke's three parameters gradient-corrected functional (B3LYP) with a polarized 6-31G (d,p) was used for the geometrical optimization and for the HOMO and LUMO levels determination. In order to limit computational time, hexyl and thiohexyl were replaced by propyl and thioethyl groups. The contours of the HOMO and LUMO orbitals and a schematic evolution of their levels are shown in Figure 2.

The optimized structures of **EEa-c** present a quasi planar anti conformation, the distortional angle between the two EDOT units is about  $10^\circ$ . The thioalkyl or alkyl groups of **EEa-c** point in a quasi-perpendicular direction. It can be noted that the conformations adopted by the alkylsulfanyl groups confirm the structures revealed by X-ray diffractions of **EEb**. The energy levels of the HOMO and LUMO of compounds **EEa-c** present values of the HOMO ranging between -4.96 eV for **EEb** and -4.57 eV for **EEa** while the LUMO are ranging from -1.23 eV

for **EEb** to -0.68 eV for **EEa**. Thus the alkyl groups impart a slightly more electron donor character than the thioalkyl ones. The sulphur atoms of the thioalkyl groups do not present any orbital contribution to the HOMO level. Only the inductive electron withdrawing effect of the sulphur atoms influences the HOMO levels of **EEb** and **EEc** which are stabilized compared to **EEa**. In contrast, as they contribute to the LUMO orbital levels, sulphur atoms have a greater influence on its stabilization. This explains the decrease of bandgap with sulphur addition.

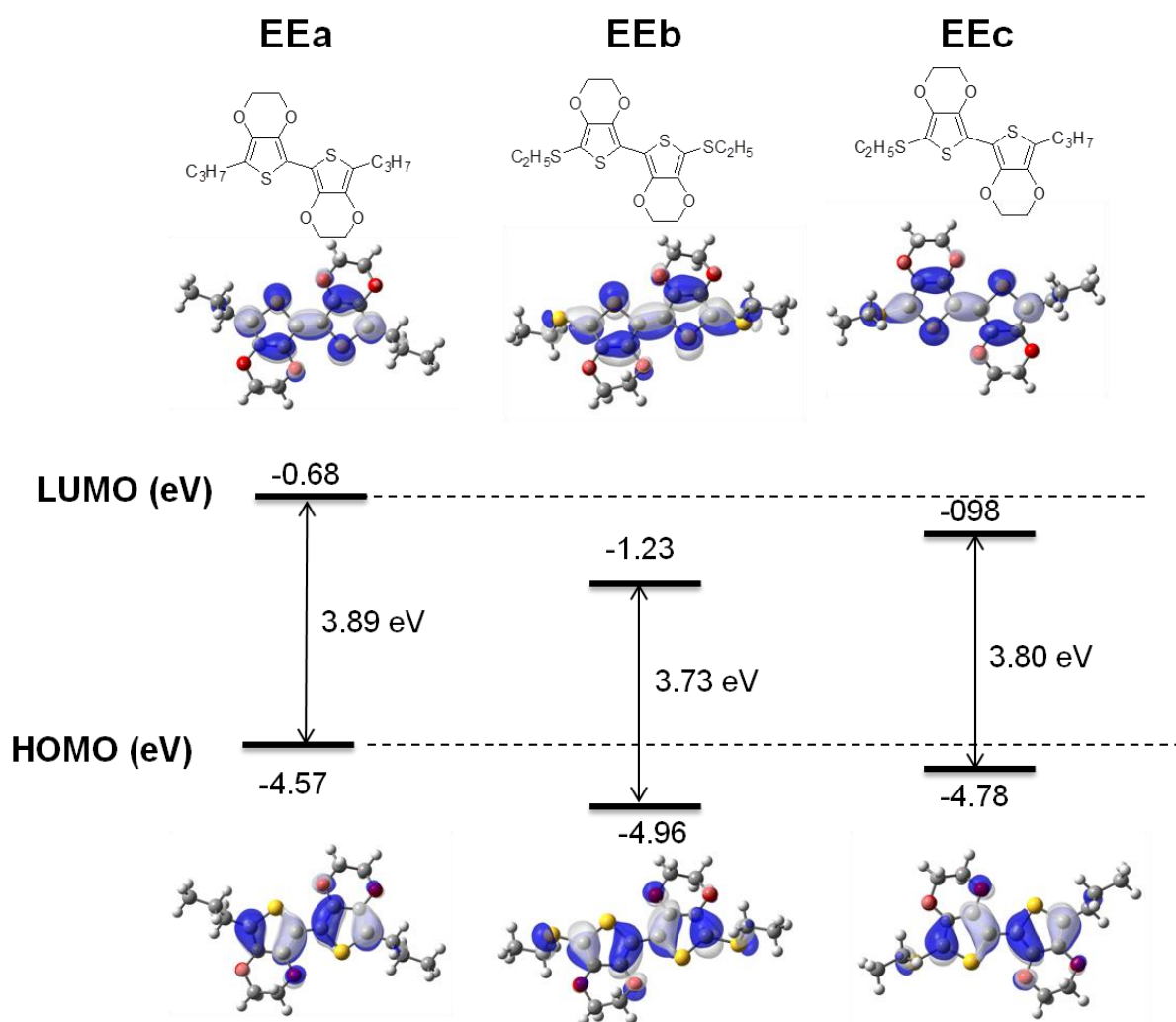


**Figure 2:** Calculated HOMOs and LUMOs energy levels of **EEa**, **EEb** and **EEc**.

The electrochemical properties of compounds were analyzed by cyclic voltammetry and the oxidation potentials are gathered in Table 1. The nature of the end capping substituents has a strong influence on the electrochemical behavior of compounds upon oxidation and influences

both oxidation potential and processes reversibility. The values of the first oxidation potential  $E_{ox1}$  follow the sequence given by the HOMO levels, namely **EEa** < **EEc** < **EEb** indicating well the more electron donor character of the alkyl groups. The cyclic voltammograms of **EEa** and **EEb** are presented in Figure 3. Regardless of the scan rate, the cyclic voltammogram of **EEa** always presents an irreversible oxidation peak at 0.65 V even with a scan rate up to  $1.0 \text{ V.s}^{-1}$ . Such behavior indicates a rapid evolution of the radical cation at the electrode.<sup>22</sup> By contrast **EEb** presents two reversible oxidation waves at 0.74 V and 0.89 V even at low scan rate ( $10 \text{ mV/s}$ ) corresponding to the formation of very stable radical cation and dication species. For compound **EEc** (Figure 4) end capped both by hexyl and hexylsulfanyl substituents the cyclic voltammogram with a scan rate of  $100 \text{ mV.s}^{-1}$  shows a first partially reversible oxidation peak at 0.70 V followed by a second less intense reversible wave at 1.00 V. By increasing the rate of the scan in potential, the reversibility of the first peak increases while the intensity of the second peak rises. Thus for a scan rate of  $500 \text{ mV.s}^{-1}$  the cyclic voltammogram of **EEc** presents two reversible oxidation waves respectively at 0.76 V and 1.02 V.

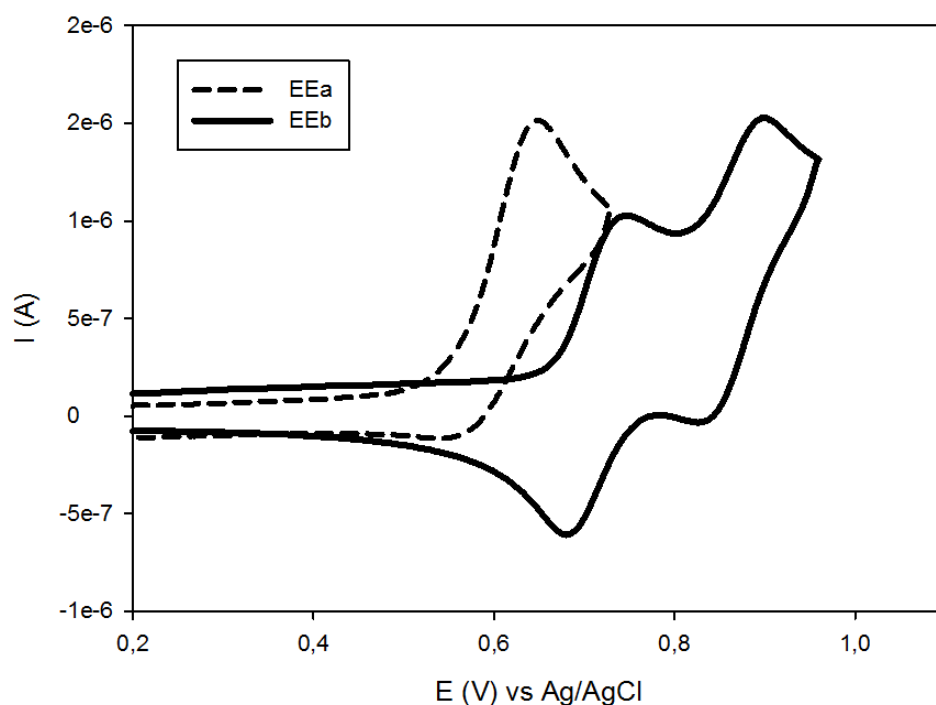


**Figure 3:** CV trace of **EEa** (dotted line) and **EEb** (solid line)  $10^{-3} \text{ mol.L}^{-1}$  in  $0.1 \text{ M Bu}_4\text{NPF}_6$  in  $\text{CH}_2\text{Cl}_2$ ,  $\nu = 100 \text{ mV.s}^{-1}$ .

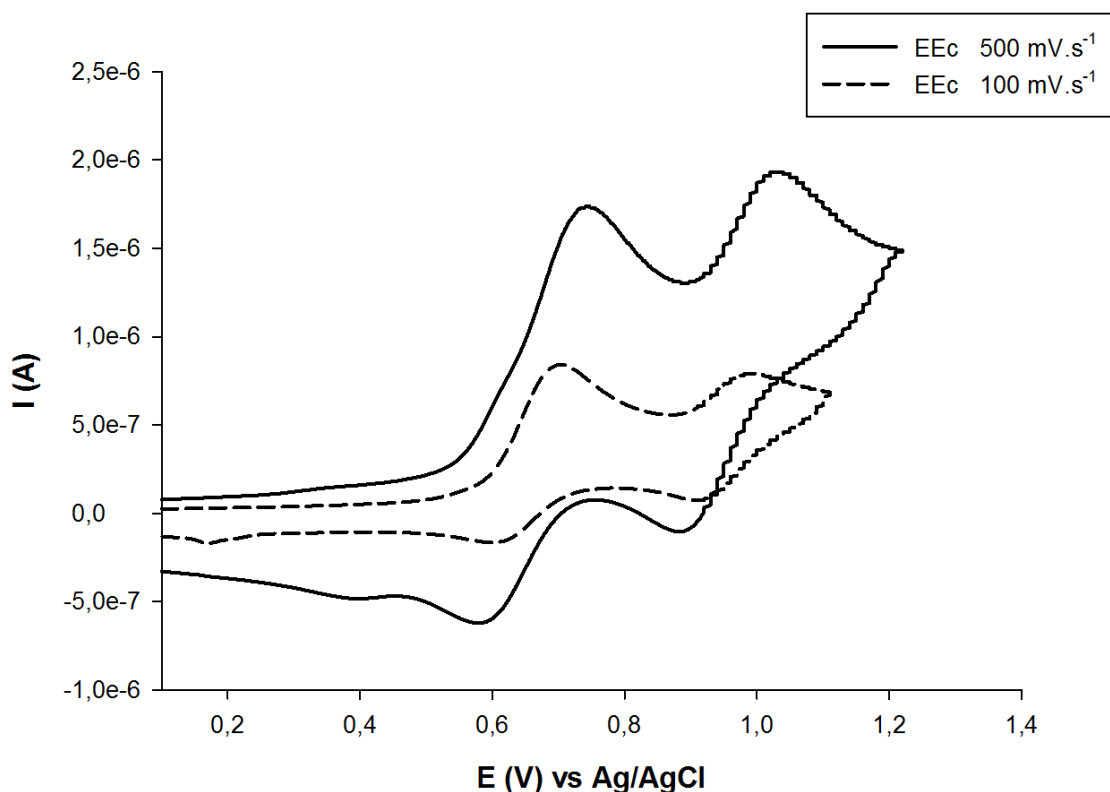


**Figure 4:** CV trace of **EEc**  $10^{-3}$  mol.L $^{-1}$  in 0.1 M Bu $_4$ NPF $_6$  in CH $_2$ Cl $_2$ ,  $v = 100$  mVs $^{-1}$  (dotted line) or  $v = 500$  mVs $^{-1}$  (solid line).

This strong difference in the electrochemical behaviors can be interpreted by a more or less rapid dimerization process of the radical cations **EEa** $^{+}$  and **EEc** $^{+}$ . As already demonstrated by Heinze et al., the hexyl chains substituted on the  $\alpha$  position of the thiophene units does not suppress the possibility of the radical cation to dimerize leading to a dication specie named  $\sigma$ -dimer. By contrast the sulfur atoms of hexylsulfanyl groups stabilize the oxidized species of **EEb** leading to reversible processes. In the intermediate case of **EEc**, due to the presence of an hexylsulfanyl chain, the kinetic of the dimerization process of the radical cation **EEc** $^{+}$  is slower than for **EEa** $^{+}$ . Thus for medium to fast scan rates, the radical cation does not dimerize before the potential reaches  $E_{ox2}$  allowing the formation of the stable dication **EEc** $^{2+}$ .

In absorption spectroscopy, the three compounds present well resolved fine structures with the presence of two distinct maxima indicating increased rigidity of the conjugated skeleton due to S---O intramolecular interactions.<sup>9, 30</sup> The end capping groups have a slight effect on the bandgap calculated from the lowest energy bands ( $\lambda_{0-0}$ ) what is consistent with the theoretical calculation. The progressive replacement of the alkyl by thioalkyl groups induces a decrease of the optical bandgap from 3.55 eV for **EEa** to 3.37 eV for **EEb**.



The stability of the different species (cation radical, dication and  $\sigma$ -dimer) resulting from the oxidation of **EEa** and **EEb** were examined by UV-visible/NIR spectroscopy in  $\text{CH}_2\text{Cl}_2$ . The visible/NIR spectra of a solution of **EEb** ( $10^{-4} \text{ mol.L}^{-1}$ ) at room temperature recorded during the addition of a  $\text{NOSbF}_6$  solution are shown in Figure 5. The oxidation of **EEb** into cation radical is marked by a slow color change from yellow to purple. The stepwise addition of  $\text{NOSbF}_6$  provokes both a decrease of the neutral state band at 380 nm and the emergence of two new main bands at 510 nm and 920 nm (D1 and D2) which are characteristic of the formation of radical cation. The band which emerges at 450 nm when the concentration in radical cation raises may correspond to the formation of  $\pi$ -dimers. Such  $\pi$ -dimers were composed of a face to face interaction of the  $\pi$ -orbitals of the radical cations as already described for oligothiophene derivatives.<sup>5, 31, 32</sup> The evolution of the absorbance at  $\lambda = 510 \text{ nm}$  ( $A_{510}$ ) in function of the addition of  $\text{NOSbF}_6$  at constant concentration in **EEb** is presented in Figure S1 in supplementary information. The maximum of  $A_{510}$  is obtained when 1 equivalent of  $\text{NOSbF}_6$  is added as expected for the formation of a radical cation. The further addition of oxidant leads to the decrease of  $A_{510}$  to reach a plateau at 2 equivalents of  $\text{NOSbF}_6$ . The bands of the cation radical are replaced by a weak broad band at 480 nm assigned to the dication (Figure 6).

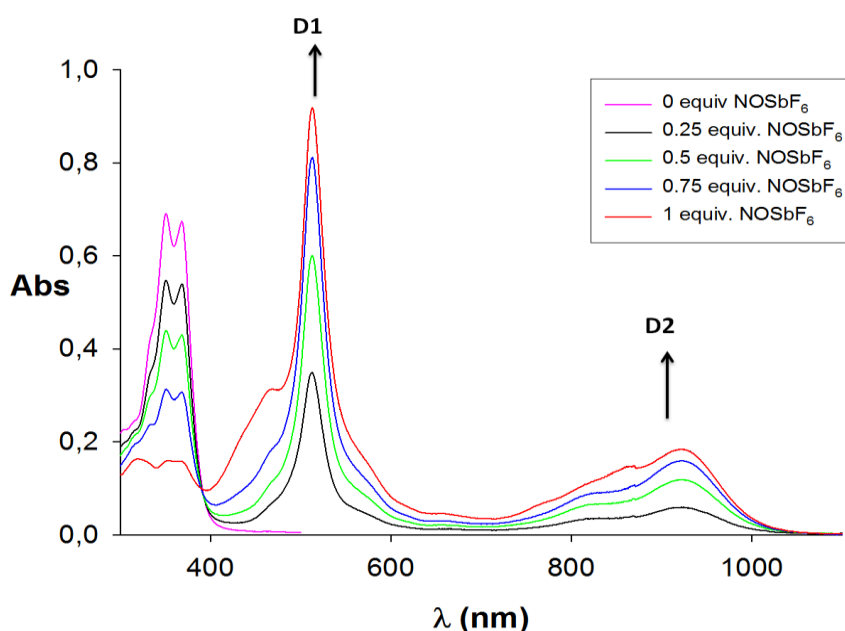


**Figure 5:** Stepwise addition of  $\text{NOSbF}_6$  in  $10^{-4} \text{ M}$  solution of **EEb** in  $\text{CH}_2\text{Cl}_2$

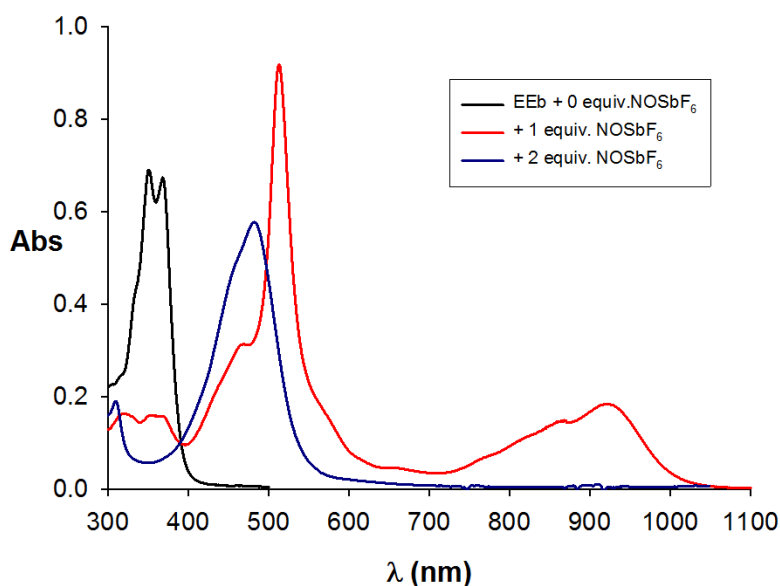
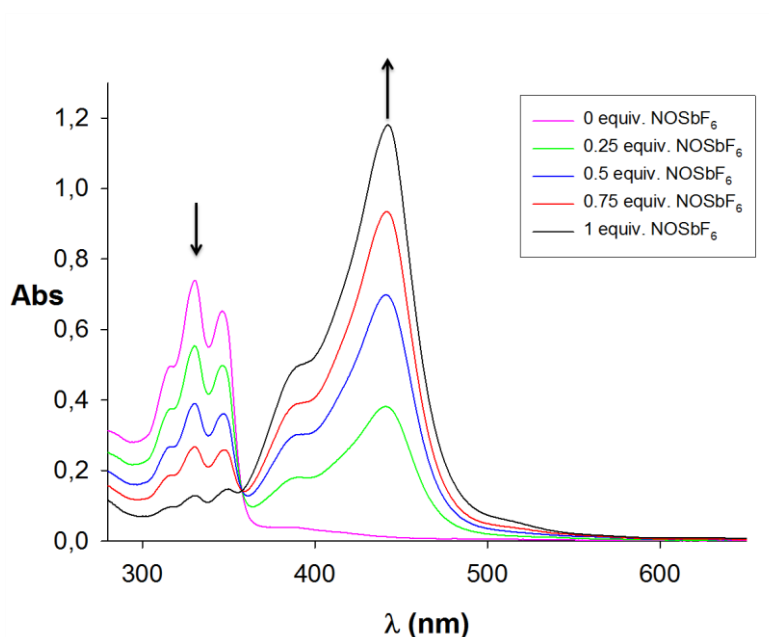


Figure 6: UV-vis-NIR spectra of **EEb** (black), **EEb<sup>+•</sup>** (red) and **EEb<sup>2+</sup>** (blue) 10<sup>-4</sup> M in CH<sub>2</sub>Cl<sub>2</sub>.

For compound **EEa**, the oxidation is very fast and leads to an orange solution. As shown in Figure 7, the oxidation leads to the emergence of an intense band at 440 nm. The absorbance at  $\lambda = 440$  nm ( $A_{440}$ ) measured during the stepwise addition of oxidant reaches a plateau from 1 equivalent of NOSbF<sub>6</sub> (Figure S1). Moreover, the absence of band above 600 nm shows that the specie obtained by addition of 1 eq of NOSbF<sub>6</sub> is not a radical cation but may correspond to  $\sigma$ -dimer (**EEa**)<sub>2</sub><sup>2+</sup>.<sup>27</sup> This dimer is not oxidized by the addition of an excess of oxidant.

The reduction of the  $\sigma$ -dimer was analyzed by addition of hydrazine (Figure 8). The gradual addition of hydrazine leads to the disappearance of the bands of (**EEa**)<sub>2</sub><sup>2+</sup> (430nm) together with the regeneration of the neutral species. The total recovery of starting material needs a slight excess of reducing reagent. Immediately, a new band at 400nm emerges. This later, observed during the reduction disappears rapidly what underlines the non stability of the corresponding species. We postulate that the reduction of the  $\sigma$ -dimer with hydrazine leads to an intermediate which could correspond to the radical cation of the  $\sigma$ -dimer (**EEa**)<sub>2</sub><sup>+•</sup>.



**Figure 7:** Stepwise addition of  $\text{NOSbF}_6$  in  $10^{-4}$  M solution of **EEa** in  $\text{CH}_2\text{Cl}_2$

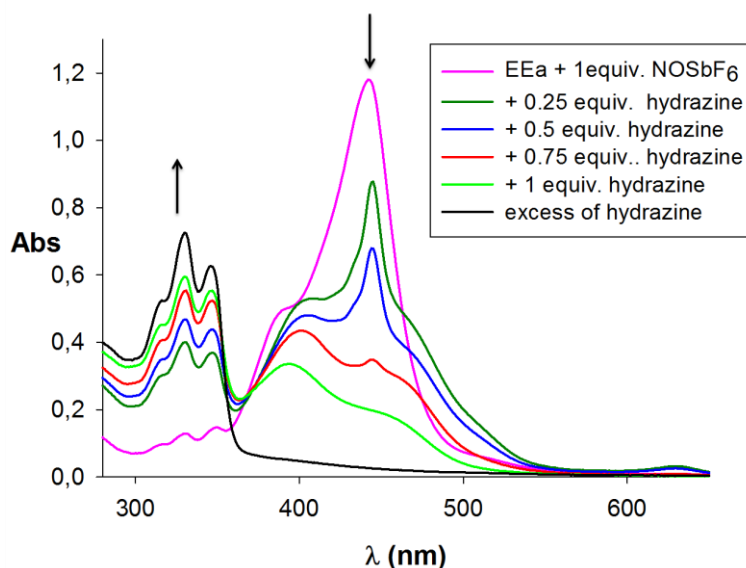
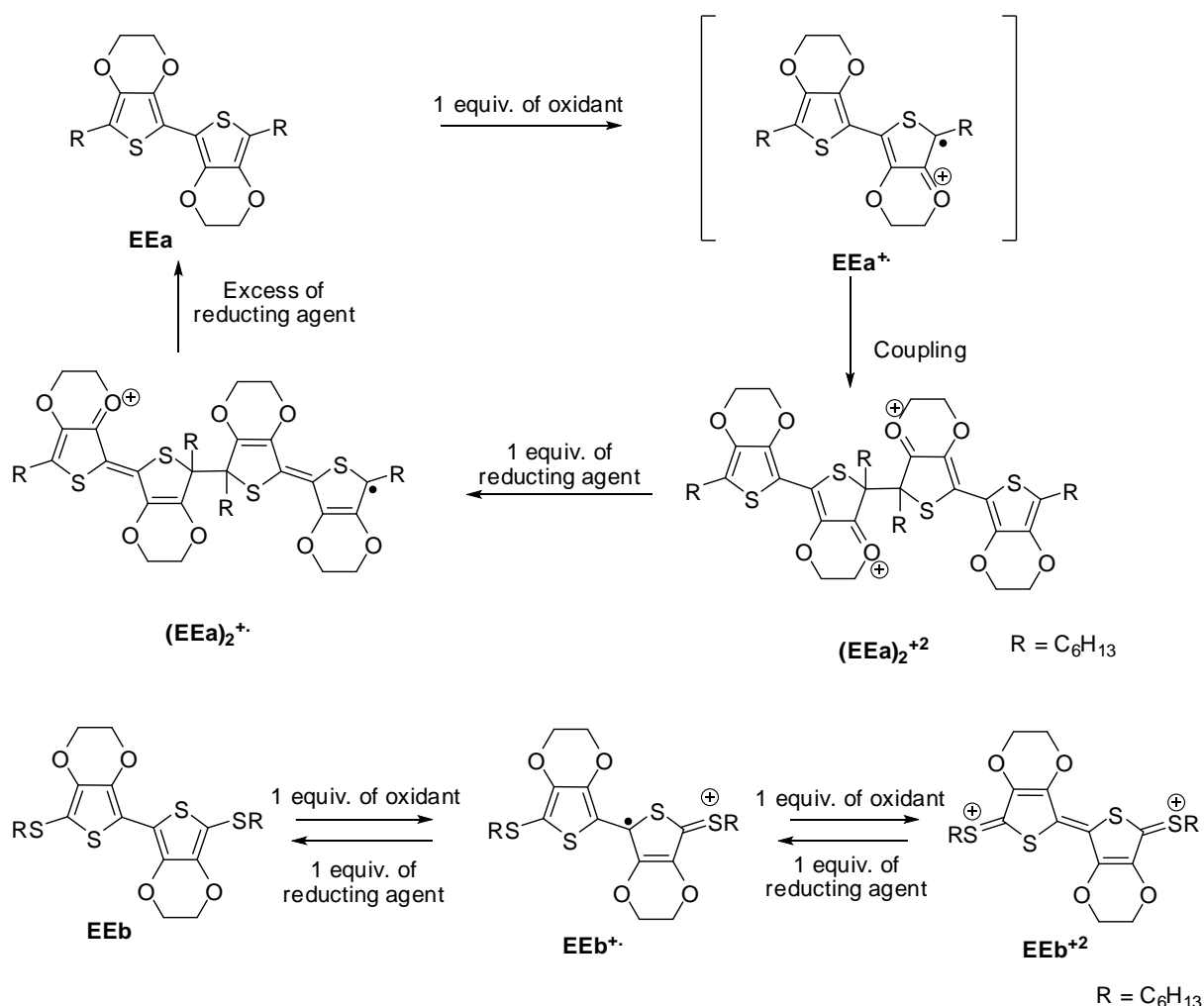


**Figure 8:** Stepwise addition of hydrazine in a solution of **EEa** + 1 eq of  $\text{NOSbF}_6$

Scheme 2 summarizes the two different oxidation processes observed for **EEa** and **EEb**. In accordance with the results described by Heinze, the radical cation **EEa**<sup>•+</sup> undergoes a fast coupling reaction leading to  $\sigma$ -dimer (**EEa**)<sub>2</sub><sup>2+</sup>. The hexyl chain exerts an inductive donor effect that enhances the spin density on the terminal carbon. This effect, in addition to that of the ethylenedioxy groups, leads to a highly reactive radical. The coupling reaction is reversible. The oxidation step is rapid while the reduction process carries out in two slower steps, with the formation of the radical cation (**EEa**)<sub>2</sub><sup>•+</sup> as intermediate. For compound **EEb**

substituted with hexysulfanyl groups the mesomeric effect of the sulfur atoms stabilize the cation radical and dication species by localizing the positive charges on the extremity of the molecules (Scheme 2). Thus for the radical cation the coupling reaction leading to the  $\sigma$ -dimer is inhibited. For **EEc**, the presence of only one hexysulfanyl chain does not suppress but decreases the kinetic of the coupling reaction.



**Scheme 2:** Oxidation and reduction processes postulated for **EEa** and **EEb**

The impact of the sulfur atom of the alkylsulfanyl groups on the oxidized states is well evidenced by theoretical calculation. The optimized structures of the dications have been performed by using the same parameters (B3LYP, 6.31G(d,p)) as for the neutral states. For the three compounds **EEa-c**, the optimized structures present a quinoidic character with in particular a shortening of the central bond linking the two EDOT units as expected for an ethylenic bond (see ESI). Although the thioalkyl groups of **EEb** and **EEc** pointed in a

perpendicular direction of the plane defined by the EDOT moieties for the neutral states, in the dicationic state, they are in the extension of the plane of the EDOT units. Moreover the length of the C-S bonds decrease relatively to the neutral state and the sulfur atoms present an orbital contribution indicating a participation of the sulfur atoms to the delocalization of the positive charges (see supplementary information).

## Conclusion

A series of bis-EDOT derivatives end capped with n-hexyl and n-hexylsulfanyl groups have been synthesized. The comparison of their oxidation processes, by cyclic voltammetry and UV/Vis spectroscopy, shows that the sulfur atoms of the alkylsulfanyl groups increase the stability of the cation radical state. Thus, while the radical cation of n-dihexyl derivative **EEa** presents a rapid evolution, the substitution of an hexyl by an hexylsulfanyl group in **EEc** increases the stability of the radical cation and allows to reach the dication state. The substitution of the two hexyl groups in **EEb** leads to a high stability of the radical cation and dication. The UV/Vis spectroscopy confirms the stability of the two oxidation states of **EEb** and shows that the fast evolution of radical cation of **EEa** corresponds to a  $\sigma$ -dimerization process. The dimerization is reversible but presents a slow reduction process involving several steps. The sulfur atoms introduced on the external positions of EDOT cores participate to the electronic delocalization in cationic and dicationic states and prevent the dimerization process of the radical cation, thus leading to a high stability of the oxidized states.

## Experimental

### General

*Electrochemical measurements:* Cyclic voltammetry was performed in a three-electrode cell (5 mL) equipped with a platinum millielectrode of  $10^{-2}$  cm<sup>2</sup> and a platinum wire counter electrode. An Ag/AgCl electrode checked against the ferrocene/ferricinium couple before and after each experiment was used as reference. All experiments were carried out in CH<sub>2</sub>Cl<sub>2</sub> solution (HPLC grade) with tetrabutyl ammonium hexafluorophosphate deaerated by argon bubbling at 298K.

*Electronic absorption measurements:* UV/Vis/near-IR experiments have been performed with Perkin-Elmer Lambda 19 NIR spectrometer. Solvents (HPLC grade) were deoxygenated

before use. The oxidation of the neutral donors in solution was accomplished by adding solutions of nitrosonium hexafluoroantimonate (NOSbF<sub>6</sub>) from a micro-syringe.

### Synthetic procedures

Bis-EDOT<sup>33</sup> and **EEa**<sup>22</sup> were prepared as already described.

#### 5,5'-dihexylsulfanyl-2,2'-bis(3,4-ethylenedioxiophene) **EEb**

A solution of bis-EDOT (400 mg, 1.42 mmol) in dry THF (80 mL) was cooled to - 20 °C and 2.1 mL of *n*-BuLi (1.6 M, 2.4 eq.) was added dropwise. The mixture was stirred for 30min, and 100 mg of dry sulfur (2.2 eq.) were added. After 30 min of stirring 800 µL of bromohexane (4.25 mmol) were added and the yellow resulting solution was allowed to warm at room temperature and stirred overnight. The solvent was evaporated and the residue, dissolved in diethyl ether, was successively washed with saturated aqueous NH<sub>4</sub>Cl solution and water. The organic phase was dried over MgSO<sub>4</sub> and the solvent was evaporated. The resulting orange oil was chromatographed on a column of silica gel (CH<sub>2</sub>Cl<sub>2</sub>/Petroleum ether, 1/1) to give **EEb** as pale yellow solid (300 mg, 42%).

**EEb**: mp 118°C, <sup>1</sup>H NMR (CDCl<sub>3</sub>) 0.88 (t, 6H, J = 6.9 Hz), 1.24-1.39 (m, 6H), 1.54-1.62 (m, 4H), 2.71 (t, 4H, J = 7.4 Hz), 4.31 (s, 8H). <sup>13</sup>C NMR (CDCl<sub>3</sub>) 14.1, 22.6, 28.5, 28.9, 31.7, 38.1, 64.8, 65.0, 105.4, 112.2, 136.8, 143.4. MS (MALDI-TOF): m/z calcd for C<sub>24</sub>H<sub>34</sub>O<sub>4</sub>S<sub>4</sub> 514.1, found 514.1. Elemental analysis calcd (%) for C<sub>24</sub>H<sub>34</sub>O<sub>4</sub>S<sub>4</sub>: C 56.00, H 6.66, O 12.43; found: C 55.26, H 6.57, O 12.44.

#### 5-hexylsulfanyl-5'-hexyl-2,2'-bis(3,4-ethylenedioxiophene) **EEc**

A solution of bis-EDOT (500 mg, 1.77 mmol) in dry THF (80 mL) was cooled to - 20 °C and 2.42 mL of *n*BuLi (1.6 M, 2.2 equiv.) was added dropwise. The mixture was stirred for 30min, and 55 mg of dry sulfur (1.1 eq.) were added. After 30 min of stirring, 1 mL of bromohexane (5.31 mmol) was added and the yellow resulting solution was allowed to warm at room temperature and stirred overnight. The solvent was evaporated and the residue, dissolved in diethyl ether, was successively washed with saturated aqueous NH<sub>4</sub>Cl solution and water. The organic phase was dried over MgSO<sub>4</sub> and the solvent was evaporated. The residue was purified by chromatography on a column of silica gel (CH<sub>2</sub>Cl<sub>2</sub>/Petroleum ether, 1/1) to give **EEc** (300 mg, 35%) as a pale yellow solid. Compound **EEb** was isolated as side product in 15 % yield.

**EEc**: mp 129°C. <sup>1</sup>H NMR (CDCl<sub>3</sub>) 0.88 (m, 6H), 1.27-1.41 (m, 12H), 1.57-1.77 (m, 4H), 2.73 (t, 2H, J = 7.4 Hz), 2.88 (t, 2H, J = 7.4 Hz), 4.33 (s, 8H). <sup>13</sup>C NMR (CDCl<sub>3</sub>) 14.1 (2), 22.6 (2), 28.2, 28.3, 28.8, 28.9, 29.5, 31.4 (2), 38.1, 39.3, 64.8, 64.9, 65.0, 65.1, 106.4, 107.3, 111.9,

114.5, 136.6, 137.3, 143.2, 144.2. MS (MALDI-TOF):  $m/z$  calcd for  $C_{24}H_{34}O_4S_3$  482.2, found 482.1; Elemental analysis calculated (%) for  $C_{24}H_{34}O_4S_3$ : C 59.72, H 7.10, O 13.26; found: C 59.28, H 7.07, O 13.34.

#### Crystal Data and structure refinement for compound **EEb**

Single crystal of **EEb** were mounted on an Enraf-Nonius MACH3 diffractometer with graphite monochromator and Mo  $K\alpha$  ( $\lambda = 0.71073 \text{ \AA}$ ) at  $T = 293 \text{ K}$ . The data collections were performed with the  $\omega/2\theta$  scan technique. The crystal structures were solved by direct method (SIR) and refined by full matrix least square techniques using SHELX97 software. The H atoms were found by Fourier difference synthesis.

$C_{24}H_{34}O_4S_4$ , Mw = 514.75, triclinic, P-1,  $a = 4.919(2) \text{ \AA}$ ,  $b = 7.285(1) \text{ \AA}$ ,  $c = 18.574(2) \text{ \AA}$ ,  $\alpha = 84.19(1)^\circ$ ,  $\beta = 86.42(1)^\circ$ ,  $\gamma = 84.08(2)^\circ$ ,  $V = 657.7(3) \text{ \AA}^3$ ,  $Z = 1$ ,  $\rho_{\text{calc}} = 1.300 \text{ g.cm}^{-3}$ , 4216 reflections collected in the  $2.82\text{--}30.04^\circ$   $\theta$  range, 3803 independent reflections with  $I > 2\sigma(I)$  converged to  $R = 0.0571$  and  $wR2$  (all data) = 0.176 with 146 parameters, GOF = 1.032.

CCDC reference number 1026287.

#### References

1. G. Barbarella, M. Melucci and G. Sotgiu, *Adv. Mater.*, 2005, **17**, 1581-1593.
2. A. Pron, P. Gawrys, M. Zagorska, D. Djurado and R. Demadrille, *Chem. Soc. Rev.*, 2010, **39**, 2577-2632.
3. A. Mishra, C.-Q. Ma and P. Bauerle, *Chem. Rev.*, 2009, **109**, 1141-1276.
4. J. Cao, J. W. Kampf and M. D. Curtis, *Chem. Mater.*, 2003, **15**, 404-411.
5. J. Cao and M. D. Curtis, *Chem. Mater.*, 2003, **15**, 4424-4430.
6. M. Turbiez, N. Hergu  , P. Leriche and P. Fr  re, *Tetrahedron Lett.*, 2009, **50**, 7148.
7. Y. H. Wijsboom, Y. Sheynin, A. Patra, N. Zamoshchik, R. Vardimon, G. Leitus and M. Bendikov, *J. Mater. Chem.*, 2011, **21**, 1368-1372.
8. G. J. McEntee, P. J. Skabara, F. Vilela, S. Tierney, I. D. W. Samuel, S. Gambino, S. J. Coles, M. B. Hursthouse, R. W. Harrington and W. Clegg, *Chem. Mater.*, 2010, **22**, 3000.
9. M. Turbiez, P. Fr  re, M. Allain, C. Videlot, J. Ackermann and J. Roncali, *Chem.-Eur. J.*, 2005, **11**, 3742-3752.
10. A. Bolduc, S. Dufresne and W. G. Skene, *J. Mater. Chem.*, 2010, **20**, 4820-4826.
11. C.-Y. Liu, H. Zhao and H.-H. Yu, *Org. Lett.*, 2011, **13**, 4068-4071.
12. D. Demeter, T. Rousseau and J. Roncali, *RSC Advances*, 2013, **3**, 704-707.

13. N. Cai, Y. Wang, M. Xu, Y. Fan, R. Li, M. Zhang and P. Wang, *Adv. Func. Mater.*, 2013, **23**, 1846-1854.
14. P. Gao, H. N. Tsao, C. Yi, M. Grätzel and M. K. Nazeeruddin, *Adv. Ener.Mater.*, 2014, **4**, 1301485.
15. L. Fillaud, G. Trippé-Allard and J. C. Lacroix, *Org. Lett.*, 2013, **15**, 1028-1031.
16. D. Cortizo-Lacalle, C. T. Howells, S. Gambino, F. Vilela, Z. Vobecka, N. J. Findlay, A. R. Inigo, S. A. J. Thomson, P. J. Skabara and I. D. W. Samuel, *J. Mater. Chem.*, 2012, **22**, 14119-14126.
17. M. E. Mulholland, D. Navarathne, S. Khedri and W. G. Skene, *New J. Chem.*, 2014, **38**, 1668-1674.
18. J. Roncali, P. Blanchard and P. Frère, *J. Mater. Chem.*, 2005, **15** (16), 1589-1610.
19. I. Tabakovic, T. Maki, L. L. Miller and Y. Yu, *Chem. Commun.*, 1996, 1911-1912.
20. R. G. Hicks and M. B. Nodwell, *J. Am. Chem. Soc.*, 2000, **122**, 6746-6753.
21. J. Casado, M. Z. Zgierski, R. G. Hicks, D. J. T. Myles, P. M. Viruela, E. Orti, M. Carmen Ruiz Delgado, V. Hernandez and J. T. Lopez Navarrete, *J. Phys. Chem. A*, 2005, **109**, 11275.
22. M. Turbiez, P. Frère and J. Roncali, *J. Org. Chem.*, 2003, **68**, 5357-5360.
23. M. Kondratenko, A. G. Moiseev and D. F. Perepichka, *J. Mater. Chem.*, 2011, **21**, 1470-1478.
24. Y. Yu, E. Gunic, B. Zinger and L. L. Miller, *J. Am. Chem. Soc.*, 1996, **118**, 1013-1018.
25. P. Tschuncky, J. Heinze, A. Smie, G. Engelmann and G. Kossmehl, *J. Electroanal. Chem.*, 1997, **433**, 223 - 226.
26. A. Smie, A. Synowczyk, J. Heinze, R. Alle, P. Tschuncky, G. Gotz and P. Bauerle, *J. Electroanal. Chem.*, 1998, **452**, 87-95.
27. J. Heinze, H. John, M. Dietrich and P. Tschuncky, *Synth. Met.*, 2001, **119**, 49-52.
28. J. Heinze, C. Willmann and P. Bauerle, *Angew. Chem. Int. Ed.*, 2001, **40**, 2861-2864.
29. A. Merz, S. Anikin, B. Lieser, J. Heinze and H. John, *Chem.- Eur. J.*, 2003, **9**, 449-455.
30. P. Leriche, M. Turbiez, V. Monroche, P. Frère, P. Blanchard, P. J. Skabara and J. Roncali, *Tetrahedron Lett.*, 2003, **44**, 649-652.
31. E. Levillain and J. Roncali, *J. Am. Chem. Soc.*, 1999, **121**, 8760-8765.
32. A. Neudeck, P. Audebert, L. Guyard, L. Dunsch, P. Guiriec and P. Hapiot, *Acta Chem. Scand.*, 1999, **53**, 867 - 875.
33. A. K. Mohanakrishnan, A. Hucke, M. A. Lyon, M. V. Lakshmikantham and M. P. Cava, *Tetrahedron*, 1999, **55**, 11745-11754.